European Journal of Medicinal Chemistry 44 (2009) 3986–3993

Contents lists available at ScienceDirect

European Journal of Medicinal Chemistry

journal homepage: http://www.elsevier.com/locate/ejmech

Original article

Synthesis, spectroscopic characterization, X-ray structure and evaluation of binding parameters of new triorganotin(IV) dithiocarboxylates with DNA

Zia-ur Rehman [a,c], Afzal Shah [a], Niaz Muhammad [a], Saqib Ali [a,*], Rumana Qureshi [a], Auke Meetsma [b], Ian Sydney Butler [c]

[a] Department of Chemistry, Quaid-i-Azam University, Islamabad 45320, Pakistan
[b] Crystal Structure Center, Chemical Physics, Zernike, Institute for Advanced Materials, University of Groningen, Nijenborgh 4, NL-9747 AG Groningen, The Netherlands
[c] Department of Chemistry, McGill University, 801 Sherbrook Street West, Montreal, Quebec, Canada H3A2K6

ARTICLE INFO

Article history:
Received 30 December 2008
Received in revised form
9 April 2009
Accepted 16 April 2009
Available online 3 May 2009

Keywords:
Triorganotin(IV) dithiocarboxylates
Spectroscopy
X-ray diffraction
DNA interaction
Binding constant

ABSTRACT

Three new triorganotin(IV) dithiocarboxylates (**1**–**3**) with general formula R_3SnL, where $R = C_4H_9$ (**1**), C_6H_{11} (**2**), C_6H_5 (**3**) and L = 4-(4-nitrophenyl)piperazine-1-carbodithioate, have been synthesized and characterized by elemental analysis, Raman, FT-IR, multinuclear NMR (^1H, ^{13}C and ^{119}Sn) and mass spectrometry. The crystal structure of complex **3** confirmed distorted trigonal-bipyramidal geometry around Sn atom. The interaction of compounds **1**–**3** with DNA was investigated by cyclic voltammetry (CV) and UV–vis spectroscopy. The positive peak potential shift in CV and hypochromic effect in spectroscopy evidenced intercalative mode of interaction. The results indicate that the binding affinity varies in this sequence: **1** > **3** > **2**.

© 2009 Published by Elsevier Masson SAS.

1. Introduction

There has been much interest in recent years in studying the interaction of coordination complexes with DNA due to their potential candidature as anti-tumor agents after the discovery of clinically used cisplatin. However, the serious negative side effects of platinum-pharmaceuticals diverted the attention of the researchers to non-platinum chemotherapeutics with positive, low or no side effects. Among these organotins received utmost attention on account of their potential apoptotic inducing character and high therapeutic index [1–3]. Their DNA binding studies are of paramount importance in the development of new anticancer agents and DNA molecular probes. The interaction of small molecules with the DNA is of three types: (i) electrostatic interaction with the anionic phosphate of DNA backbone, (ii) intercalation into the stacked base pairs of DNA and (iii) groove binding. The prerequisite for useful applications of coordination complexes requires their direct binding to DNA through intercalation, in which the compound causes unwinding of the local structure of DNA, which culminates in the damage of the DNA storage, transcription and genetic transformation machinery. Therefore, extensive studies have been focused on modifying the intercalative ligand [4].

Organotin(IV) dithiocarboxylates are the subject of intensive investigations due to their structural diversity, anti-tumor activity and biological applications [5,6]. The coordination with the Sn atom depends not only on factors such as structure of the organic groups, but also whether the 1,1-dithiolate moiety behaves as monodentate or bidentate. Based on these factors triorganotin(IV) dithiocarboxylates either exhibit tetrahedral or trigonal-bipyramidal geometry. In continuation of our work, and as part of ongoing study of dithiocarboxylate complexes of organotin(IV) and of their coordination chemistry [7,8], we have synthesized, characterized three triorganotin(IV) derivatives of 4-(4-nitrophenyl) piperazine-1-carbodithioate and evaluated their binding parameters with DNA. The structure of the ligand salt is demonstrated in Scheme 1(a).

2. Results and discussion

2.1. Proposed mechanism of ligand and complexes *1*–*3* synthesis

The nucleophilic attack of 4-(4-nitrophenyl)piperazine on carbon disulfide gave 4-(4-nitrophenyl)piperazine-1-carbodithioic acid as intermediate which undergoes acid–base reaction with unreacted 4-(4-nitrophenyl)piperazine to gave 4-(4-nitrophenyl)

* Corresponding author. Tel.: +925190642208; fax: +92512873869.
E-mail address: drsa54@yahoo.com (S. Ali).

0223-5234/$ – see front matter © 2009 Published by Elsevier Masson SAS.
doi:10.1016/j.ejmech.2009.04.031

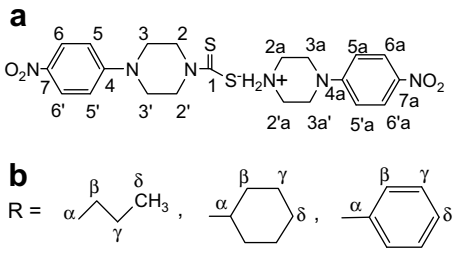

Scheme 1. Numbering scheme of ligand-salt and organic groups.

piperazinium 4-(4-nitrophenyl)piperazine-1-carbodithioate (L-salt). The reaction of the ligand salt with R_3SnCl ($R = C_4H_9$, C_6H_{11} and C_6H_5) gave R_3SnL and 4-(4-nitrophenyl)piperazinium chloride as shown in Scheme 2. This mechanism has been proposed on the basis of multinuclear NMR (^1H and ^{13}C) study of the ligand and successfully analyzing the crystal structure of the by-product, 4-(4-nitrophenyl) piperazinium chloride and is shown in Fig. 3.

2.2. Vibration spectra

In Raman spectra, the appearance of Sn–S peak in the region of 362–384 cm^{-1} is an indication of the formation of complexes. Very sharp Sn–C peak was observed at 515 and 510 cm^{-1} in complexes **1** and **2**, whereas in triphenyltin(IV) derivative a weak Sn–C peak was observed at 263 cm^{-1}.

Of particular interest in the IR spectra are the C–N, C–S stretching frequencies. Both can be used to differentiate between mono and bidentate modes of coordination of 1,1-dithiolate moiety. The presence of single band in the region of 900–1000 cm^{-1} due to υ(C–S) is an indication of bidentate character whereas the presence of two bands with separation value > 20 cm^{-1} suggests that ligand bonding is monodentate [9]. In our present study the appearance of two bands for C–S, in complexes **1** and **2**, is in agreement with monodentate bonding of 1,1-dithiolate moiety with Sn. The unsplitting of the C–S peak in compound **3** is an indicative of bidentate coordination of dithiocarboxylate group, and is consistent with crystal structure of **3**. The stretching vibration peaks of the C–N, in the studied complexes, were located at 1478–1497 cm^{-1}. These values lie between the range of C–N single bonds (1250–1360 cm^{-1}) and C=N double bond (1640–1690 cm^{-1}) which is an indication of partial double bond character in C–N bond [6]. The appearance of new peaks at 514 cm^{-1} and 510 cm^{-1} in compounds **1** and **2** is assigned to Sn–C.

2.3. NMR spectra

The ^1H NMR spectra of the investigated compounds were recorded in DMSO. The assignment of the proton resonances was made by their peak multiplicity, intensity pattern and comparison of the integration values of the protons with the expected composition. The disappearance of duplication peak pattern due to 4-(4-nitrophenyl)piperazinium ion and appearance of proton signals for the organic groups attached to Sn confirmed the formation of complexes **1**–**3**.

In the spectra of complexes **1** and **2**, the protons of piperazine moiety of the ligand showed two multiplets (4.15 and 3.62 ppm) in the aliphatic region while aromatic part of the ligand gave two doublets due to two non-equivalent sets of protons. The tributyl- and tricyclohexyl-groups attached to the Sn illustrated proton resonances at 1.75–0.089 ppm and 2.04–1.24 ppm, respectively. Difficulty in obtaining the ^nJSn–H coupling in these two complexes due to complex nature of the proton resonances of tributyl- and tricyclohexyl-groups attached to the Sn, renders almost no information about the geometry around Sn atom. In the case of triphenyltin derivative of the ligand, the proton spectrum is informative regarding the geometry around the Sn. The signals for

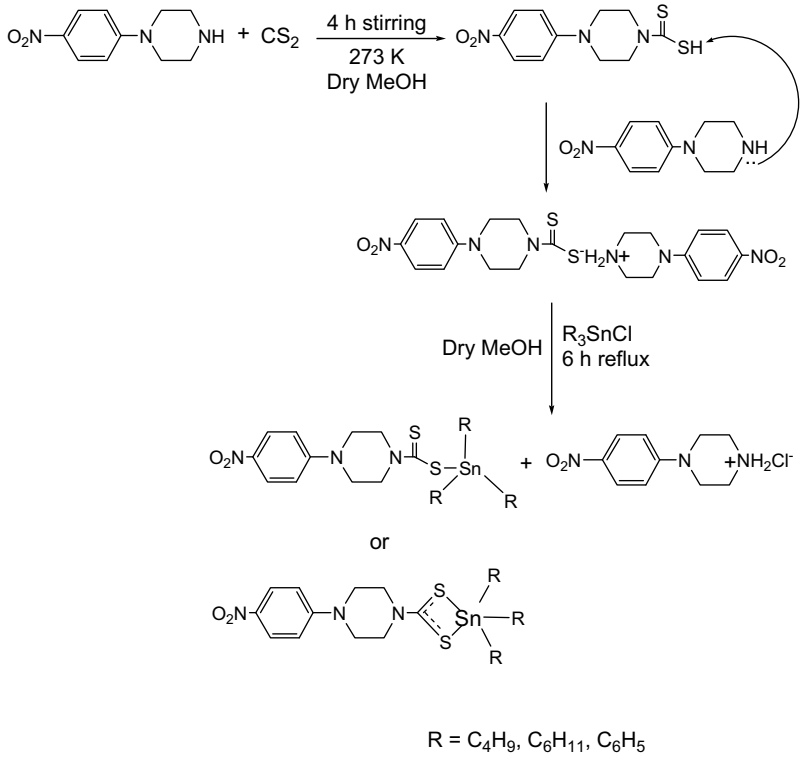

Scheme 2. Synthetic mechanism of ligand-salt and complexes.

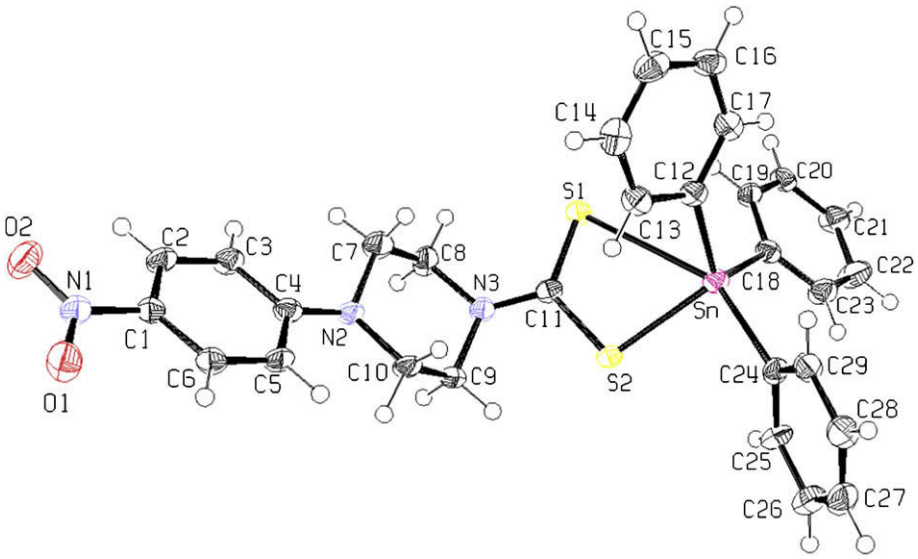

Fig. 1. ORTEP drawing of Ph_3SnL (**3**) with atomic numbering scheme.

protons of the phenyl groups attached to the Sn were distinguished into two sets. The *ortho* protons were observed at down field (7.76 ppm) and those for *meta* and *para* protons at upfield (7.39 ppm). In addition, the difference in chemical shift resonance between *ortho* and *meta* and *para* (0.37 ppm) is an indication of anisobidentate bonding of 1,1-dithiolate moiety in solution. All these observations are in agreement with the previously reported literature for a series of triphenyltin dithiocarboxylates [10]. Almost no significant change was observed in the aromatic and piperazine protons of ligand moiety in the ^{1}H spectrum of the complex **3**.

The ^{13}C NMR chemical shifts due to butyl, cyclohexyl and phenyl groups, attached to Sn atom, were observed at positions comparable to the other similar compounds [11,12]. The ^{13}C NMR chemical shifts due to the 'CS_2' carbon atom in the investigated complexes were found in the range 200.1–195.9 ppm. Coordination of the Sn atom in triorganotins has been related to the ^1J(^{119}Sn–^{13}C) coupling constant. In compounds **1** and **2** the ^1J(^{119}Sn–^{13}C) coupling constant observed was 346.6 Hz (107.2°) and 330 Hz (105.7°) which is in agreement with analogous four-coordinated organotin derivatives [13].

The mono or bidentate bonding of the ligand to the organotin moiety, in the complexes, was further confirmed by ^{119}Sn NMR spectroscopy. It has been reported that δ (^{119}Sn) values (in ppm) for organotin(IV) dithiocarboxylate with four-coordinate Sn vary from +120 to −145 ppm while ^{119}Sn signal in the range of −150 to −250 ppm corresponds to five-coordinate Sn [14]. In case of complexes **1** and **2**, the ^{119}Sn spectra gave only a sharp singlet at 39.6 ppm and −17.5 ppm confirmed the formation of a single species with the tetrahedral geometry around Sn while complex **3** gave signal (−195 ppm) in the region for five-coordinated Sn atom.

2.4. Mass spectra

Mass-spectral data for **1**–**3** showed rich ion distributions but our interest lies in Sn containing ions. These ions were easily and quantitatively identified from the characteristic isotopic peak pattern for Sn [15]. The mass-spectral data reported here are related to the principal isotope ^{120}Sn. Complexes **1**–**3** show no molecular ion (M^+) as is generally the case for main group organometallic

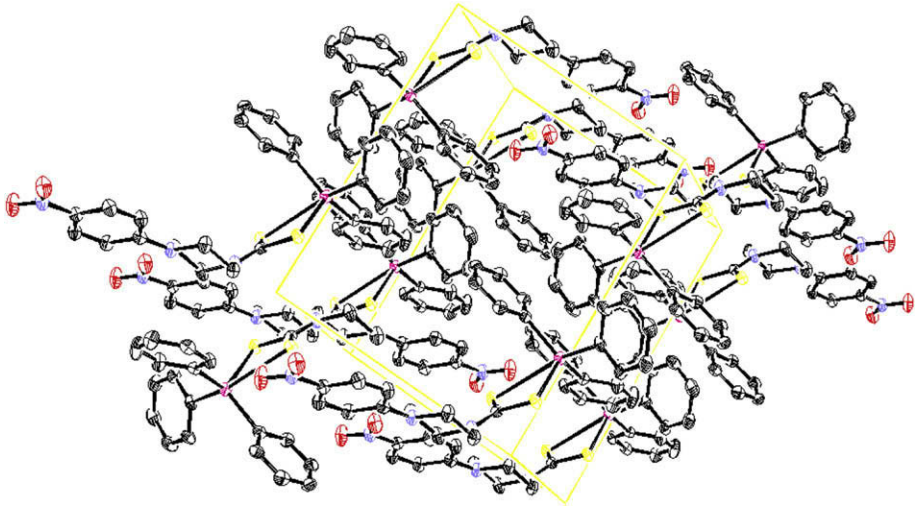

Fig. 2. Packing of molecules in a unit cell of Ph_3SnL (**3**).

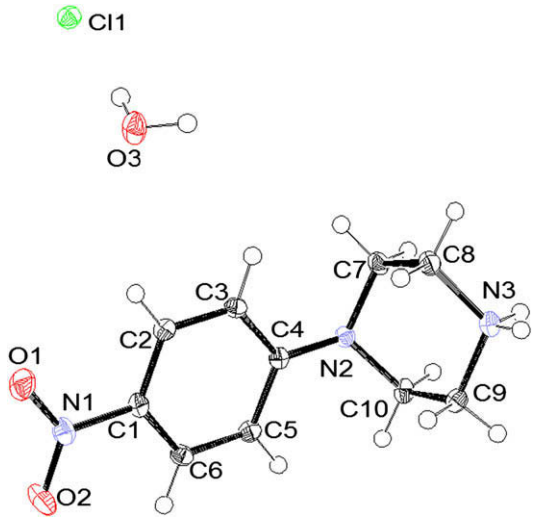

Fig. 3. ORTEP drawing of 4-(4-nitrophenyl)piperazinium chloride with atomic numbering scheme.

compounds, however, for compounds **1–3**, the different fragments observed are consistent with structures proposed on the basis of other spectroscopic techniques.

2.5. X-ray structure of compound (*3*)

The molecular structure and packing of molecules in a unit cell of compound **3** are depicted in Figs. 1 and 2, respectively, while crystal data and selected bond lengths and bond angles are given in Tables 1 and 2, respectively. The geometry around the Sn atom is distorted trigonal-bipyramidal, the equatorial plane being defined by the two carbons of the phenyl groups and a sulfur atom of the dithiocarboxylate ligand. According to Addison et al., the geometry around the Sn atom can be characterized by the value of $\tau = (\beta - \alpha)/60$ [16], where β is the largest of the basal angles around the Sn atom. For compound **3**, it is S1–Sn–C24 = 152.35°. The second largest of the basal angles around the Sn atom, α for compound **3** is S2–Sn–C18 = 118.29°. The angle values $\alpha = \beta = 180°$ correspond to a square-pyramidal geometry, and the value of $\alpha = 120°$ corresponds to perfectly trigonal-bipyramidal geometry. Thus, the τ value is equal to zero for a perfect square-pyramidal and unity for a perfect trigonal-pyramidal [16,17]. The calculated τ value for the complex is 0.57. The value indicates a highly distorted trigonal-bipyramidal arrangement around Sn atom with C24 from a phenyl group and the S1 from the dithiocarboxylate in the axial positions while C12 and C18 from two phenyl groups and S2 in the plane positions. The sum of the equatorial angles, [S2–Sn–C12 = 108.73 (13)°, S2–Sn–C18 = 118.29 and C12–Sn–C18 = 115.57 (11)°], is 342.59° instead of the ideal 360°. Being a part of chelate, the angle S2–Sn–S1 is not 90° but only 62.27°, so the S1 cannot occupy exactly the corresponding *trans* apical position of C24 and the angle between the apical groups is 152.35°. The Sn–C bond length, C24 = 2.151 (5) Å, is very similar to equatorial ones, Sn–C18 = 2.135 (5) Å and in agreement with Sn–C values reported for $Ph_3SnS_2CN(CH_3)(C_4H_9)$ [18]. Finally, the C–S bond lengths are characteristic of the 1,1-dithiolate moiety and are intermediate between the values expected for single and double bonds [19].

Table 1
Crystal data and structure refinement parameter for Ph_3SnL (**3**).

Empirical formula	$C_{29}H_{27}N_3O_2S_2Sn$
Formula mass	632.39
Crystal system	Triclinic
Space group, no.	*P*-1, 2
a (Å)	9.546 (2)
b (Å)	10.986 (2)
C (Å)	13.650 (3)
α (°)	91.966 (3)
β (°)	98.752 (3)
γ (°)	107.833 (3)
V (Å^3)	1341.9 (5)
Z (*Z*′)	2 (1)
Crystal habit/size (mm)	Block/0.55 × 0.33 × 0.24
T (K)	100 (1)
μ (Mo K$\bar{\alpha}$) (cm^{-1})	11.4
Total reflections	11783
Independent reflections	6288
All	
For $F_o \geq 4.0\ \sigma(F_o)$	5541
$R(F) = \sum(\|\|F_o\| - \|F_c\|\|)/\sum\|F_o\|$	0.0388
For $F_o > 4.0\ \sigma(F_o)$	
$wR(F^2) = [\sum[w(F_o^2 - F_c^2)^2]/\sum[w(F_o^2)^2]]^{1/2}$	0.1195
Goodness-of-fit	1.239
θ range for data collections (°)	2.51–28.28
Data/restraints/parameters	6288/0/334

Table 2
Selected bond lengths (Å) and angles (°) for Ph_3SnL (**3**).

Sn–S2	2.4419 (14)	Sn–C24	2.151 (5)
Sn–C12	2.114 (5)	S–C11	1.674 (5)
Sn–C18	2.135 (5)	S2–C11	1.760 (4)
Sn–S1	3.179		
S2–Sn–C12	108.73 (13)	S1–Sn–C12	77.54
S2–Sn–C18	118.29 (11)	S1–Sn–C18	87.53
S2–Sn–C24	90.15 (12)	S1–Sn–C24	152.35
C12–Sn–C18	115.57 (18)	S1–Sn–S2	62.27
C12–Sn–C24	112.44 (18)	S1–Sn–C24	152.35
C18–Sn–C24	108.96 (18)	S1–C11–S2	120.0 (3)
Sn–C12–C13	120.3 (4)	Sn–C12–C17	120.3 (4)
Sn–C18–C19	123.0 (3)	Sn–C18–C23	118.7 (4)
Sn–C24–C25	119.6 (3)	Sn–C24–C29	121.2 (4)
Sn–S2–C11	99.33 (15)	Sn–S1–C11	76.65

2.6. Cyclic voltammetry of compounds *1–3* binding to DNA

The cyclic voltammetric behavior of 3 mM compound **1** and the effect of addition of different concentrations of DNA on its electrochemical response in 10% aqueous dimethylsulphoxide (DMSO),

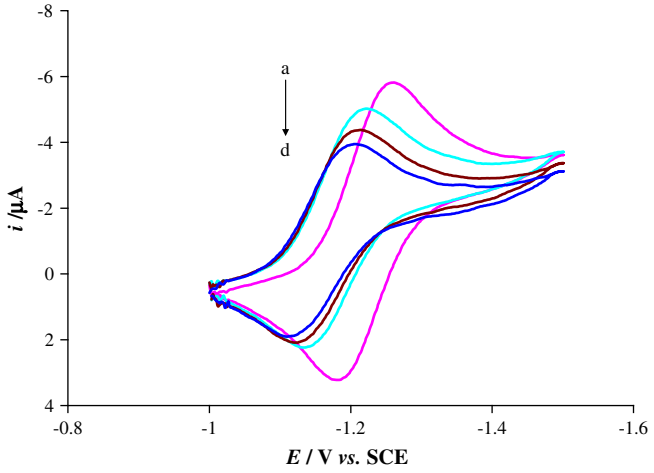

Fig. 4. Cyclic voltammograms of 3.00 mM **1** in 10% aqueous DMSO with 0.1 M TBAP as supporting electrolyte in the absence (a) and presence of 3.0×10^{-5} (b), 6.5×10^{-5} (c) and 1.05×10^{-4} M DNA (d) at 25 °C temperature. Glassy carbon electrode (0.071 cm^2) was used as working electrode and all potentials were reported *vs.* SCE at 100 mV s^{-1} scan rate.

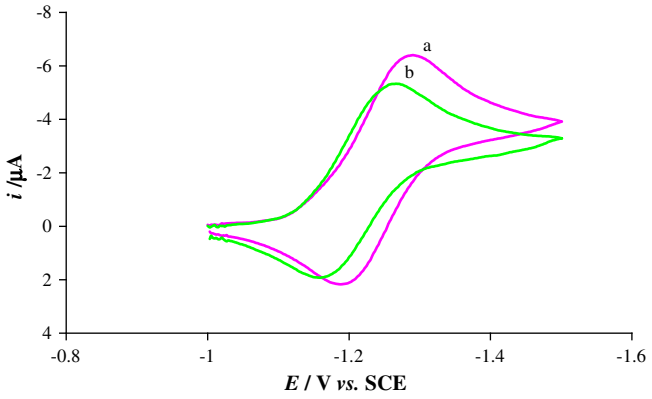

Fig. 5. Cyclic voltammograms of 3.00 mM **2** in 10% aqueous DMSO with 0.1 M TBAP as supporting electrolyte in the absence (a) and presence of 3.2×10^{-5} M DNA (b) at 25 °C temperature. Glassy carbon electrode (0.071 cm^2) was used as working electrode and all potentials were reported *vs.* SCE at 100 mV s^{-1} scan rate.

containing 10^{-1} M tetra-n-butylammonium perchlorate as supporting electrolyte at 100 mV s^{-1} are depicted in Fig. 4. The free drug registered a single cathodic peak at −1.261 V and an anodic peak at −1.181 V upon scan reversal, in the potential range of −1.0 to −1.5 V. The appearance of these two peaks is an indication of interconversion of Sn^{+4} to Sn^{+2} and vice versa during the whole process [19]. The peak potentials separation of 80 mV, greater than the ideal value of 60 mV for a fully reversible redox process may be due to kinetic complications. With the stepwise addition of DNA, a gradual shift of the peak potential in positive direction accompanied with the decrease in peak current was observed. The positive shift in peak potentials is suggestive of intercalative mode of binding in which the complex inserts itself into the stacked base pairs domain of DNA [20]. The decay in peak current is attributed to the decrease in the concentration of the free complex due to the formation of heavy drug–DNA association complex with concomitant lower diffusion coefficient.

Typical CV behavior of **2** with and without DNA is shown in Fig. 5. The redox behavior of compound **2** without DNA featured oxidation and reduction at −1.293 and −1.193 V respectively. By the addition of 3.2×10^{-5} M DNA, a 13.38% drop in cathodic peak current and 22 mV peak potential shift in the positive direction were observed. These observations unambiguously reflect the intercalation of the complex into the double helical structure of

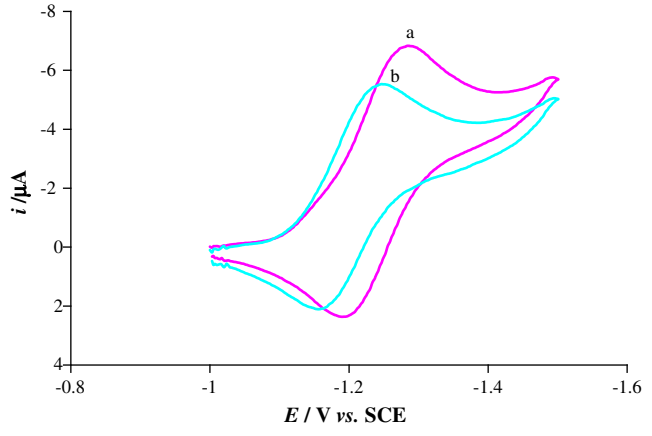

Fig. 6. Cyclic voltammograms of 3.00 mM **3** in 10% aqueous DMSO with 0.1 M TBAP as supporting electrolyte in the absence (a) and presence of 5.0×10^{-5} M DNA (b) at 25 °C temperature. Glassy carbon electrode (0.071 cm^2) was used as working electrode and all potentials were reported *vs.* SCE at 100 mV s^{-1} scan rate.

Table 3
Voltammetric parameters of compounds **1**–**3** in the absence and presence of DNA.

Substance	ν/V s^{-1}	[DNA]/ μM	E_{pa}/V	E_{pc}/V	E_f°/V	D_f 10^9/ cm^2 s^{-1}	D_b 10^9/ cm^2 s^{-1}
1	0.1	0	−1.181	−1.261	−1.221	8.05	–
1–DNA	0.1	30	−1.132	−1.225	−1.178	–	7.39
2	0.1	0	−1.193	−1.293	−1.243	15.13	–
2–DNA	0.1	32	−1.161	−1.271	−1.216	–	8.86
3	0.1	0	−1.188	−1.288	−1.238	8.62	–
3–DNA	0.1	50	−1.156	−1.249	−1.202	–	5.36

DNA as electrostatic interaction with anionic phosphate backbone of DNA is evidenced by the negative peak potential shift [21]. The voltammetric behavior of compound **3** in the absence and presence of DNA (Fig. 6) is analogous to the CV behavior of compounds **1** and **2**. Peaks associated with the reduction of $Sn^{IV/II}$ and reoxidation to $Sn^{II/IV}$ appeared at −1.288 and at −1.188 V respectively. In the presence of 5.0×10^{-5} M DNA, the cathodic and anodic peaks appeared at −1.249 and −1.156 V accompanied with 19% reduction of the cathodic peak current. Such peculiar voltammetric characteristics signify intercalative interaction of compound **3** with DNA. The voltammetric parameters are given in Table 3.

The diffusion coefficients of the free (D_f) and DNA bound complexes (D_b) were determined by the application of Randles–Sevcik equation [22,23]:

$$i_p = 2.69 \times 10^5 n^{3/2} A C_o^* D^{1/2} \nu^{1/2} \quad (1)$$

where i_p is the peak current (A), A is the surface area of the electrode (cm^2), C_o^* is the bulk concentration (mol cm^{-3}) of the electroactive species, D is the diffusion coefficient (cm^2 s^{-1}), ν is the scan rate (V s^{-1}) and n is the number of electrons involved in the electron transfer reaction.

The linearity of i_p *vs.* $\nu^{1/2}$ plots in all cases indicated that the main mass transport of these complexes (in the absence and presence of DNA) to the electrode surface is controlled by diffusion step [24]. The lower diffusion coefficients of the DNA bound species are responsible for the decay of current signals in CV behavior of **1**–**3** (Figs. 4–6). The smaller slopes for the diffusion coefficient of compounds **1**–**3** in the presence of DNA could be attributed to their intercalation into DNA resulting in the formation of slowly diffusing supramolecular complexes in solution.

Based upon the decay in peak current of complexes **1**–**3** by the addition of varying concentration of DNA, the binding constants (Table 4) were calculated from the plots of 1/[DNA] *vs.* $1/(1 - i/i_o)$, according to the following equation [25]:

$$\frac{1}{[DNA]} = \frac{K(1-A)}{1 - i/i_o} - K \quad (2)$$

where, K is the association constant, i and i_o are the peak currents with and without DNA and A is the proportionality constant.

An examination of Table 4 reveals that the binding constants of the complexes **1**–**3** with DNA are greater than the K observed for similar DNA-intercalating Cr complex, $[CrCl_2(dicnq)_2]^+$, with K

Table 4
The association constants and Gibbs free energies of **1**–DNA, **2**–DNA and **3**–DNA complexes as determined by voltammetry and UV–vis spectroscopy.

Drug–DNA complex	CV		Spectroscopy	
	K/M^{-1}	$-\Delta G$/kJ mol^{-1}	K/M^{-1}	$-\Delta G$/kJ mol^{-1}
1–DNA	6.90×10^3	21.90	6.05×10^3	21.57
2–DNA	2.40×10^3	18.76	2.30×10^3	19.18
3–DNA	3.60×10^3	20.29	3.25×10^3	20.03

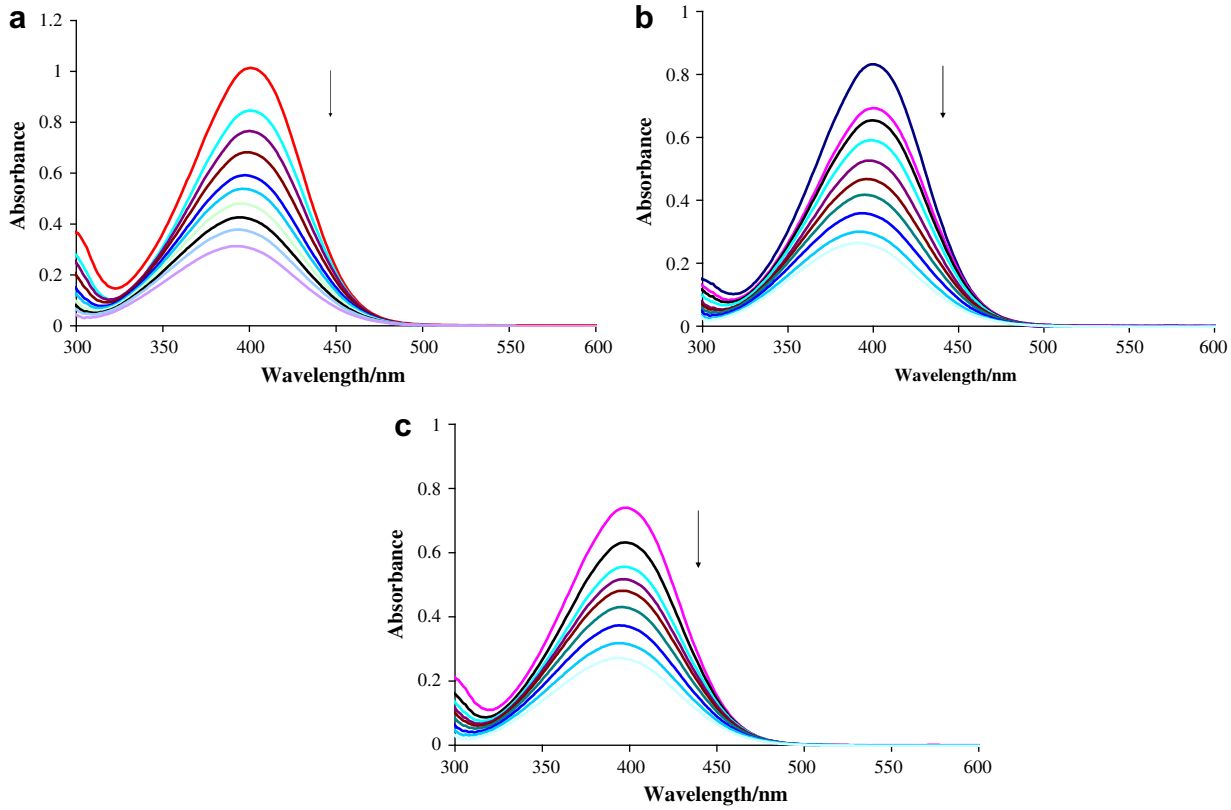

Fig. 7. Absorption spectra of 3 mM **1** in the absence (a) and presence of 2.0×10^{-5} (b), 3.0×10^{-5} (c), 4.5×10^{-5} (d), 6.0×10^{-5} (e), 7.0×10^{-5} (f), 9.0×10^{-5} (g), 1.0×10^{-4} (h), 1.15×10^{-4} (i) and 1.25×10^{-4} M DNA (j) in 10% aqueous DMSO at 25 °C. The arrow direction indicates increasing concentrations of DNA. Absorption spectra of 3 mM **2** in the absence (a) and presence of 2.0×10^{-5} (b), 2.5×10^{-5} (c), 3.5×10^{-5} (d), 4.5×10^{-5} (e), 5.5×10^{-5} (f), 6.5×10^{-5} (g), 7.5×10^{-4} (h), 8.5×10^{-4} (i) and 9.5×10^{-4} M DNA (j) in 10% aqueous DMSO at 25 °C. The arrow direction indicates increasing concentrations of DNA. Absorption spectra of 3 mM **3** in the absence (a) and presence of 2.0×10^{-5} (b), 3.5×10^{-5} (c), 4.5×10^{-5} (d), 5.5×10^{-5} (e), 6.5×10^{-5} (f), 7.5×10^{-5} (g), 9.5×10^{-4} (h) and 1.15×10^{-4} M DNA (i) in 10% aqueous DMSO at 25 °C. The arrow direction indicates increasing concentrations of DNA.

reported as 1.20×10^3 M^{-1} [26] suggests their potential candidature as chemotherapeutic agents. The rationale behind their greater affinity may be the greater intercalating ability of aromatic 4-(4-nitrophenyl)piperazine-1-carbodithioate ligand, as compared to dicnq (2,3-dicyanodipyridoquinoxaline) ligand. So an effort to further improve the binding affinity of these complexes, our current research work is concentrated on the extension of aromatic 4-(4-nitrophenyl)piperazine-1-carbodithioate system. The greater K value of **3** than **2** is due to the planar phenyl groups which can better intercalate into the double helix of DNA. The reason for greater association constant of **1** is the additional hydrophobic interaction of the butyl groups with bases of DNA [27]. The interaction of these compounds will unwind the DNA helix at the interaction sites which will lead to perturbation in the DNA replication mechanism that may culminate in the death of cancerous cells.

Table 4 further reveals that the complex–DNA adduct formation is a spontaneous process and both spectroscopic and voltammetric results agree well with each other.

2.7. Electronic absorption spectra of compounds *1–3* binding to DNA

The interactions of complexes **1–3** with DNA were further examined by UV–vis spectroscopy, to get some more clues about their mode of interaction and binding strength. The absorption spectra of **1–3** in the absence and presence of different concentrations of DNA are shown in Fig. 7. The binding of complexes **1–3** to DNA caused a progressive blue shift of 10 (401–391), 8 (400–392) and 4 nm (398–394), respectively. Such spectral characteristics are indicative of their binding to DNA. The peculiar hypochromism observed here is attributed to the intercalation of these drugs into the DNA base pairs [28]. The hypochromic effect may presumably be due to the overlapping of the electronic states of the intercalating chromophore of the ligand with the DNA bases [29].

Based upon the variation in absorbance, the association constants of these complexes with DNA were determined according to Benesi–Hildebrand equation [30]:

$$\frac{A_0}{A - A_0} = \frac{\varepsilon_G}{\varepsilon_{H-G} - \varepsilon_G} + \frac{\varepsilon_G}{\varepsilon_{H-G} - \varepsilon_G} \cdot \frac{1}{K[\mathrm{DNA}]} \quad (3)$$

where K is the association constant, A_0 and A are the absorbances of the drug and its complex with DNA, respectively, and ε_G and ε_{H-G} are the absorption coefficients of the drug and the drug–DNA complex, respectively.

The association constants, shown in Table 4, were obtained from the intercept-to-slope ratios of $A_0/(A - A_0)$ *vs.* 1/[DNA] plots.

3. Conclusions

The triorganotin(IV) derivatives of 4-(4-nitropheny)piperazine-1-carbodithioate ligand exhibit tetrahedral (**1** and **2**) or distorted trigonal-bipyramidal (**3**) geometry both in solution and in solid state. The voltammetric and spectroscopic techniques were successfully used for the evaluation of binding parameters of compounds **1–3** with DNA. The association constants estimated by UV-titration agree with the electrochemical estimates. Based upon

the decrease in current and absorption intensity the stability of adduct formation followed the order: **1** > **3** > **2**. The results of CV and UV–vis spectra indicate that all the compounds **1**–**3** intercalate into the double helix of DNA. The negative values of ΔG designate the spontaneity of complex–DNA binding.

4. Experimental protocols

4.1. Materials and methods

Reagents, Ph_3SnCl, Cy_3SnCl, Bu_3SnCl and 4-(4-nitrophenyl piperazine) were obtained from Aldrich, DMSO with 99.5% purity and CS_2 from Riedal-de-Haën; methanol was dried before use by the reported method [31]. DNA was extracted from chicken blood by Falcon method [32]. The purity of DNA was spectroscopically determined from the ratio of absorbance at 260 and 280 nm ($A_{260}/A_{280} = 1.85$). The concentration of the stock solution of DNA (2.3 mM in nucleotide phosphate, NP) was determined by monitoring the absorbance at 260 nm using the molar extinction coefficient (ε) of 6600 $M^{-1}\,cm^{-1}$. UV–vis Spectrometer; Shimadzu 1601 was used for the measurement of absorption spectra.

Microanalysis was done using a Leco CHNS 932 apparatus. Raman spectra ($\pm cm^{-1}$) were measured with an InVia Renishaw spectrometer, using argon-ion (514.5 nm) and near-infrared diode (785 nm) lasers. WiRE 2.0 software was used for the data acquisition and spectra manipulations. NMR spectra (d_6-DMSO) were obtained using Hg-300 and a Varian Unity 500-MHZ instruments. Electron impact (70 eV) mass spectra were recorded on a Kratos MS25RFA instrument. Cyclic voltammetric experiments were performed by PGSTAT 302 with Autolab GPES version 4.9 Eco Chemie, Utrecht, The Netherlands. Measurements were carried out in a conventional three electrode cell with saturated calomel electrode (SCE) from Fisher scientific company (cat no.13-639-51) as a reference electrode, a thin Pt wire of thickness 0.5 mm with an exposed end of 10 mm as the counter electrode and a bare glassy carbon electrode (GCE) with a geometric area of 0.071 cm^2 as the working electrode. Prior to experiments, the GCE was polished with 0.25 μm diamond paste on a nylon buffing pad. For electrochemical measurements the test solution was kept in an electrochemical cell (model K64 PARC) connected to the circulating thermostat LAUDA model K-4R. Argon gas was used for flushing out oxygen before every electrochemical assay. Tetra-n-butylammonium perchlorate (TBAP) purchased from Fluka (99% purity) was used as supporting electrolyte and it was further purified by recrystallization, using methanol as a solvent.

4.2. Synthesis

4.2.1. Synthesis of 4-(4-nitrophenyl)piperazinium 4-(4-nitrophenyl) piperazine-1-carbodithioate (L-salt)

Dropwise addition of CS_2 (in excess) in methanol (50 mL) to 4-(4-nitrophenyl) piperazine (5 g, 24.15 mmol) in methanol (50 mL) followed by stirring for 4 h at 0 °C gave the yellowish product. The yellow product was filtered off and was washed with diethyl ether (Yield: 4.91 g, 83%). M.p. 180–182 °C. Elemental Analysis, % Calculated (Found), for $C_{21}H_{26}N_6O_4S_2$: C, 51.41 (51.37); H, 5.34 (5.33); N, 17.13 (17. 12); S, 13.07 (13.01). Raman (cm^{-1}): 664 υ(C–S), 1210 υ(C═S), 1507 υ(C–N). IR (cm^{-1}): 1030 υ(C–S), 1478 υ(C–N). ^{1}H NMR (ppm): 8.1, 8.0 (d, $H_{6,6'6a,6'a}$, $^3J_{H-H} = 9.6$ Hz), 7.1, 6.9 (d, $H_{5,5',5a,5'a}$ $^3J_{H-H} = 9.6$ Hz). 4.42–4.39, 3.69–3.65 (m, $H_{3,3',3a,3'a}$). 3.50–3.47, 3.27–3.24 (m, $H_{2,2',2a,2'a}$). ^{13}C NMR (ppm): 213.5 (C-1), 154.9, 154.7, 138.4, 137.1, 131.3, 126.3, 114.0, 112.6 (Ar–C). 49.0, 46.3 (C-3, 3′, 3a, 3′a), 43.1, 40.9 (C-2, 2′, 2a, 2′a). EI-MS, m/z (%): $[C_{10}H_{14}N_3O_2]^+$ 208 (4.7), $[C_{10}H_{13}N_3O_2]^+$ 207 (38.7), $[C_8H_9N_2O_2]^+$ 165 (100), $[C_8H_9N_2O]^+$ 149 (4), $[C_8H_9N]^+$ 119 (19.8), $[C_6H_5]^+$ 76 (24.4).

4.2.2. Synthesis of tributylstannyl 4-(4-nitrophenyl)piperazine-1-carbodithioate (**1**)

Bu_3SnCl (0.574 g, 1.76 mmol) and L-salt (0.862 g, 1.76 mmol) were mixed in methanol (80 mL) and the mixture was refluxed for 6 h with constant stirring, the yellowish product thus obtained was filtered and recrystallized from chloroform–ethanol (Yield: 0.806 g, 80%). M.p. 130–131 °C. Elemental Analysis, % Calculated (Found), for $C_{23}H_{39}N_3O_2S_2Sn$: C, 48.26 (48.20); H, 6.87 (6.93); N, 7.34 (7.42); S, 11.20 (10.98). Raman (cm^{-1}): 651 υ(C–S), 1202 υ(C═S), 1507 υ(C–N), 515 υ(Sn–C), 362 υ(Sn–S). IR (cm^{-1}): 980, 1007 υ(C–S), 1488 υ(C–N), 514 υ(Sn–C). ^{1}H NMR (ppm): 8.12 (d, $H_{6,6'}$, $^3J_{H-H} = 9.6$ Hz), 6.76 (d, $H_{5,5'}$, $^3J_{H-H} = 9.6$ Hz), 4.36 (m, $H_{3,3'}$), 3.58 (m, $H_{2,2'}$), 1.75–1.22 (m, CH_2, $SnBu_3$), 0.89 [(t, CH_3, $SnBu_3$, $^3J = 7.2$ Hz)]. ^{13}C NMR (ppm): 199.9 (C-1), 154.1, 139, 126.3, 112.6 (C–Ar), 50.6 (C-3, 3′), 46.1 (C-2, 2′), 29.1 (C-β, $^2J_{Sn-C} = 21$ Hz), 27.35 (C-γ, $^3J_{Sn-C} = 68$ Hz), 17.8 [C-α, $^1J_{Sn-C} = 346.6/331.5$ (^{119}Sn/^{117}Sn)], 13.9 (C-δ). ^{119}Sn NMR: $\delta = 39.6$ ppm. EI-MS, m/z (%): $[C_{23}H_{39}N_3OS_2Sn]^+$ 557 (25), $[C_{19}H_{30}N_3O_2S_2Sn]^+$ 516 (80), $[C_{19}H_{30}N_3OS_2Sn]^+$ 500 (27), $[C_{19}H_{30}N_2OS_2Sn]^+$ 486 (20), $[C_{11}H_{12}N_3O_2S_2Sn]^+$ 402 (33), $[C_{11}H_{12}N_3OS_2Sn]^+$ 386 (2), $[C_{12}H_{27}Sn]^+$ 291 (11), $[C_8H_{18}Sn]^+$ 234 (5), $[C_4H_9Sn]^+$ 177 (37), $[Sn]^+$ 120 (9).

4.2.3. Synthesis of tricyclohexylstannyl 4-(4-nitrophenyl) piperazine-1-carbodithioate (**2**)

Compound **2** was prepared in the same way as **1**, using the equimolar amount of L-salt (0.519 g, 1.06 mmol) and Bu_3SnCl (0.427 g, 1.06 mmol), to gave yellow product which was recrystallized from chloroform–ethanol. (Yield: 0.483 g, 70%). M.p. 228–231 °C. Elemental Analysis, % Calculated (Found), for $C_{29}H_{45}N_3O_2S_2Sn$: C, 53.54 (53.47); H, 6.97 (7.00); N, 6.46 (6.49); S, 9.86 (9.77). Raman (cm^{-1}): 656 υ(C–S), 1200 υ(C═S), 1507 υ(C–N), 510 υ(Sn–C), 364 υ(Sn–S). IR (cm^{-1}): 988, 1009 υ(C–S), 1497 υ(C–N), 510 υ(Sn–C). ^{1}H NMR (ppm): 8.12 (d, $H_{6,6'}$, $^3J_{H-H} = 9.3$ Hz), 6.77 (d, $H_{5,5'}$, $^3J_{H-H} = 9.3$ Hz), 4.37 (m, $H_{3,3'}$), 3.58 (m, $H_{2,2'}$), 2.04–1.23 (m, SnC_6H_{11}). ^{13}C NMR (ppm): 200.1 (C-1), 154, 138.9, 126.2, 112.5 (C–Ar), 50.7 (C-3, 3′), 46.1 (C-2, 2′), 35 [(C-α), $^1J_{Sn-C} = 330$ Hz/315.1 Hz (^{119}Sn/^{117}Sn)], 32.3 (C-β, $^2J = 17.1$ Hz), 29.5 (C-γ, $^3J = 68.6$ Hz), 27.2 (C-δ). ^{119}Sn NMR: $\delta = -17.5$ ppm. EI-MS, m/z (%): $[C_{29}H_{45}N_2N_2S_2Sn]^+$ 605 (3), $[C_{23}H_{34}N_3O_2S_2Sn]^+$ 568 (45), $[C_{23}H_{34}N_2OS_2Sn]^+$ 538 (7), $[C_{17}H_{30}N_2S_2Sn]^+$ 446 (5), $[C_{15}H_{26}NS_2Sn]^+$ 404 (4), $[C_{18}H_{33}Sn]^+$ 369 (5), $[C_{13}H_{22}S_2Sn]^+$ 362 (17), $[C_9H_{15}N\,S_2Sn]^+$ 321 (63), $[C_{12}H_{22}Sn]^+$ 286 (3), $[C_6H_{11}Sn]^+$ 203 (9), $[Sn]^+$ 120 (10).

4.2.4. Synthesis of triphenylstannyl 4-(4-nitrophenyl)piperazine-1-carbodithioate (**3**)

Compound **3** was prepared in the same way as **1**, using equimolar amount of L-salt (0.862 g, 1.76 mmol) and Ph_3SnCl (0.681 g, 1.76 mmol), to gave yellow product which was recrystallized from chloroform–ethanol, yielding yellow needle like crystals (Yield: 0.9 g, 80.3%). M.p. 223–226 °C. Elemental Analysis, % Calculated (Found), for $C_{29}H_{27}N_3O_2S_2Sn$: C, 55.08 (54.99); H, 4.30 (4.37); N, 6.64 (6.69); S, 10.14 (10.06). Raman (cm^{-1}): 652 υ(C–S), 1212 υ(C═S), 1507 υ(C–N), 263 υ(Sn–C), 384 υ (Sn–S). IR (cm^{-1}): 1018 υ(C–S), 1478 υ(C–N). ^{1}H NMR (ppm): 8.07 (d, $H_{6,6'}$, $^3J_{H-H} = 9.3$), 6.89 (d, $H_{5,5'}$, $^3J_{H-H} = 9.6$), 4.15(m, $H_{3,3'}$), 3.62 (m, $H_{2,2'}$), 7.76 m (H_o, SnC_6H_5), 7.39 m ($H_{m,p}$, SnC_6H_5). ^{13}C NMR (ppm): 195.9 (C-1), 154.4, 137.5, 126.4, 112.6 (C–Ar), 51.4 (C-3, 3′), 45.5 (C-2, 2′), 143.1 (C-α), 136.9 (C-β), 129.8 (C-δ), 129.3 (C-γ). ^{119}Sn NMR: $\delta = -195$ ppm. EI-MS, m/z (%): $[C_{23}H_{22}N_3O_2S_2Sn]^+$ 556 (36), $[C_{17}H_{17}N_3O_2S_2Sn]^+$ 479 (4), $[C_{11}H_{12}N_3O_2S_2Sn]^+$ 402 (3), $[C_{11}H_{12}N_2S_2Sn]^+$ 356 (3), $[C_{18}H_{15}Sn]^+$ 351 (97), $[C_{12}H_{10}Sn]^+$ 274 (7), $[C_6H_5Sn]^+$ 197 (44), $[Sn]^+$ 120 (20).

4.3. X-ray crystallography

For compound **3** crystal, X-ray data were collected on a Bruker SMART APEX CCD diffractometer using graphite-monochromated

Mo-Kα radiation ($\lambda = 0.71073$ Å). Data collection used ϕ- and ω-scans, and a multi-scan absorption correction was applied. The structure was solved by Patterson methods and extension of the model was accomplished by direct methods applied to different structure factors using the program DIRDIF. The hydrogen atoms were generated by geometrical considerations; methyl groups were defined as rigid groups which were allowed to rotate free. Final refinement on F2 carried out by full-matrix least-squares techniques using SHELXL-97.

5. Supplementary material

Crystallographic data for the structural analysis are available from Cambridge Crystallographic Data Centre, 12 Union Road, Cambridge CB2 1EZ, UK on request, quoting the deposition numbers 698264 and 713879 for complex **3** and 4-(4-nitrophenyl)piperazinium chloride, respectively. Copies of this information may be obtained free of charge from the Director, CCDC, 12 Union Road, Cambridge, CBZ, IEZ, UK (fax: +44 1223336; e-mail: deposit@ccdc.ac.uk or www: http://www.ccdc.cam.ac.uk).

Acknowledgements

The authors are grateful to Higher Education Commission of Pakistan for financial support.

References

[1] S. Tabassum, C. Pettinari, J. Organomet. Chem. 691 (2006) 1761–1766.
[2] C. Pellerito, P. D'Agati, T. Fiore, C. Mansueto, V. Mansueto, G. Stocco, L. Nagy, L. Pellerito, J. Inorg. Biochem. 99 (2005) 1294–1305.
[3] F. Cima, L. Ballarin, Appl. Organomet. Chem. 13 (1999) 697–703.
[4] Y. Xiong, L.N. Ji, Coord. Chem. Rev. 185/186 (1999) 711–733.
[5] D.C. Menezes, F.T. Vieira, G.M. de Lima, J.L. Wardell, M.E. Cortés, M.P. Ferreira, M.A. Soares, A.V. Boas, Appl. Organomet. Chem. 22 (2008) 221–226.
[6] H.D. Yin, S.C. Xue, Appl. Organomet. Chem. 20 (2006) 283–289.
[7] Z. Rehman, S. Shahzadi, S. Ali, G.X. Jin, Turk. J. Chem. 31 (2007) 435–442.
[8] Z. Rehman, M.M. Barsan, I. Wharf, N. Muhammad, S. Ali, A. Meetsma, Inorg. Chim. Acta 361 (2008) 3322–3326.
[9] O. Jung, Y.S. Sohn, J.A. Ibers, Inorg. Chem. 25 (1986) 2273.
[10] H.O. Kalinowski, S. Berger, S. Brown, ^{13}C NMR specrtoskopie, Thieme, Stuttgart, 1984.
[11] M. Nádvorník, J. Holeček, K. Handlíř, J. Organomet. Chem. 275 (1984) 43–51.
[12] G. Eng, X. Song, Q. Duong, D. Strickman, J. Glass, L. May, Appl. Organomet. Chem. 17 (2003) 218–225.
[13] R. William, I. Verbruggen, M. Gielen, M. Biesemans, B. Mahieu, T.S.B. Baul, E.R.T. Tiekink, Organometallics 17 (1998) 5758–5766.
[14] A. Tarassoli, T. Sedaghat, B. Neumüller, M. Ghassemzadeh, Inorg. Chim. Acta 318 (2001) 15–22.
[15] P.G. Harrison, in: P.G. Harrison (Ed.), Chemistry of Tin, first ed. Blackie Academic and Professional, London, 1989, p. 105.
[16] A.W. Addison, T.N. Rao, J. Reedijk, J. Van Rijn, G.C. Verschoor, J. Chem. Soc., Dalton Trans. (1984) 1349–1356.
[17] M.N. Xanthopoulou, S.K. Hadjikakou, N. Hadjiliadis, M. Kubicki, S. Karkabounas, K. Charalabopoulos, N. Kourkoumelis, T. Bakas, J. Organomet. Chem. 691 (2006) 1780–1789.
[18] A.T. Kana, T.G. Hibbert, M.F. Mahon, K.C. Molloy, I.P. Parkin, L.S. Price, Polyhedron 20 (2001) 2989–2995.
[19] G.M. Sheldrick, W.S. Sheldrick, J. Chem. Soc. A (1970) 490–497.
[20] X. Lu, M. Zhang, J. Kang, X. Wang, L. Zhuo, H. Liu, J. Inorg. Biochem. 98 (2004) 582–588.
[21] A. Shah, A.M. Khan, R. Qureshi, F.L. Ansari, M.F. Nazar, S.S. Shah, Int. J. Mol. Sci. 9 (2008) 1424–1434.
[22] J.E.B. Randles, Trans. Faraday Soc. 44 (1948) 327–338.
[23] A. Sevcik, Collect. Czech. Chem. Commun. 13 (1948) 349–377.
[24] S. Wang, T. Penz, C.F. Yang, Biophys. Chem. 104 (2003) 239–248.
[25] G.C. Zhao, J.J. Zhu, J.J. Zhang, H.Y. Chen, Anal. Chim. Acta 394 (1999) 337–344.
[26] R. Vijayalakshmi, M. Kanthimathi, R. Parthasarathi, B. Unni Nair, Bull. Chem. Soc. Jpn. 78 (2005) 270–276.
[27] Q. Lie, P. Yang, H. Wang, M. Guo, J. Inorg. Biochem. 64 (1996) 181–195.
[28] E.C. Long, J.K. Barton, Acc. Chem. Res. 23 (1990) 271–273.
[29] R. Fukuda, S. Takenaka, M. Takagi, J. Chem. Soc., Chem. Commun. (1990) 1028–1030.
[30] M.S. Ibrahim, I.S. Shehatta, A.A. Al-Nayeli, J. Pharm. Biomed. Anal. 28 (2002) 217–225.
[31] W.F.L. Armarego, C. Chai, Purification of Laboratory Chemicals, fifth ed. Butterworth, Oxford, 2003.
[32] J. Sambrook, E.F. Fritsch, T. Maniatis, Molecular Cloning: A Laboratory Manual, second ed. Cold Spring Harbour Laboratory Press, New York, 1989.